Assessment of Arctic Sea Ice in the CMIP6 Historical Simulations

Younjoo Lee[1] (ylee1@nps.edu), M. Watts[1], W. Maslowski[1], J. Clement Kinney[1], A. Craig[1], R. Osinski[2]

[1]Naval Postgraduate School, Monterey, CA; [2]Institute of Oceanology, Polish Academy of Sciences, Sopot, Poland

ABSTRACT: The response of Arctic sea ice to a warming climate is a critical indicator in climate modeling, as studied in earth system models (ESMs), including the models from the Coupled Model Intercomparison Project Phase 6 (CMIP6). Our comprehensive analysis evaluates the historical representation of sea ice against satellite observations, the Pan-Arctic Ice Ocean Modeling and Assimilation System, and the Regional Arctic System Model. We found that, while the CMIP6 multi-model mean captures the mean annual cycle and the 1979–2014 sea ice trends, individual models demonstrate substantial variability in spatial distribution and sea ice decline rates. Notably, 40% of the CMIP6 models and 13% of the ensemble members depict the observed trends and acceleration in sea ice area (SIA) decline. However, simulations of sea ice volume (SIV) present a larger spread and uncertainty, suggesting a need for improved observational constraints. Our findings reveal pronounced regional model biases and errors in ice edge and thickness, particularly in marginal and shelf seas, highlighting the models' limitations in capturing key physical processes potentially tied to oceanic forcing. The sea ice trend analysis indicates that models with higher ocean heat transport better simulate sea ice declines, hinting at an emergent constraint related to ice-ocean interactions and the necessity for enhanced modeling of processes like frazil ice growth. Therefore, accurate projections of Arctic climate change are required to identify model deficiencies, refine our understanding at the process level, and possibly enhance model physics.

1. Background and Motivation

❑ **CMIP6 models have a wide range of uncertainty in the spatial distribution of sea ice**

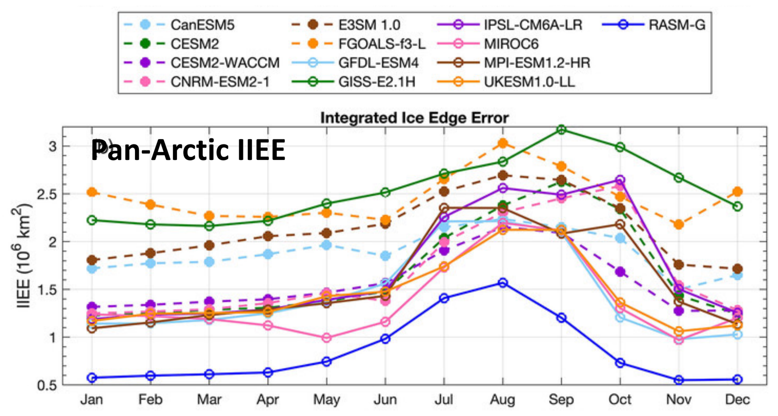

$$IIEE=\int_A|S_{model}(x,y)-S_{obs}(x,y)|dxdy$$

Figure 1. Pan-Arctic mean (1980-2014) integrated ice-edge error (IIEE, Goessling et al. 2016) for CMIP6 models and RASM-G (Fig. 7b in Watts et al. 2012).

❑ **Modeled sea ice thickness is more sensitive to model physics compared to sea ice extent/area.**

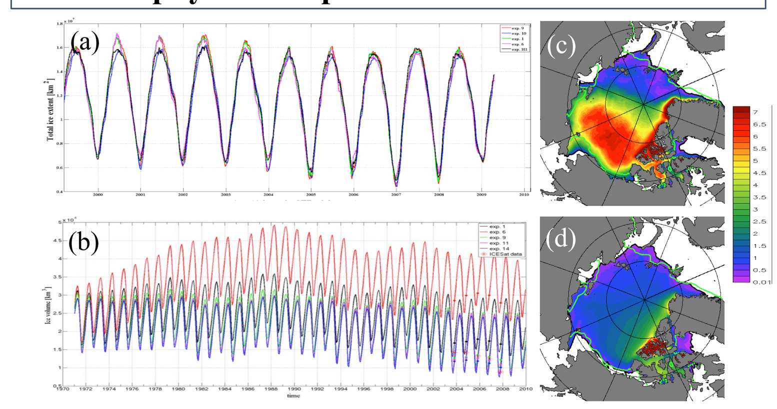

Figure 2. Timeseries of sea ice (a) extent and (b) volume from 5 RASM experiments. The 2000-2004 mean September sea ice thickness distribution (m) from (c) 'red' and (d) 'blue' experiments.

2. Regional Arctic System Model

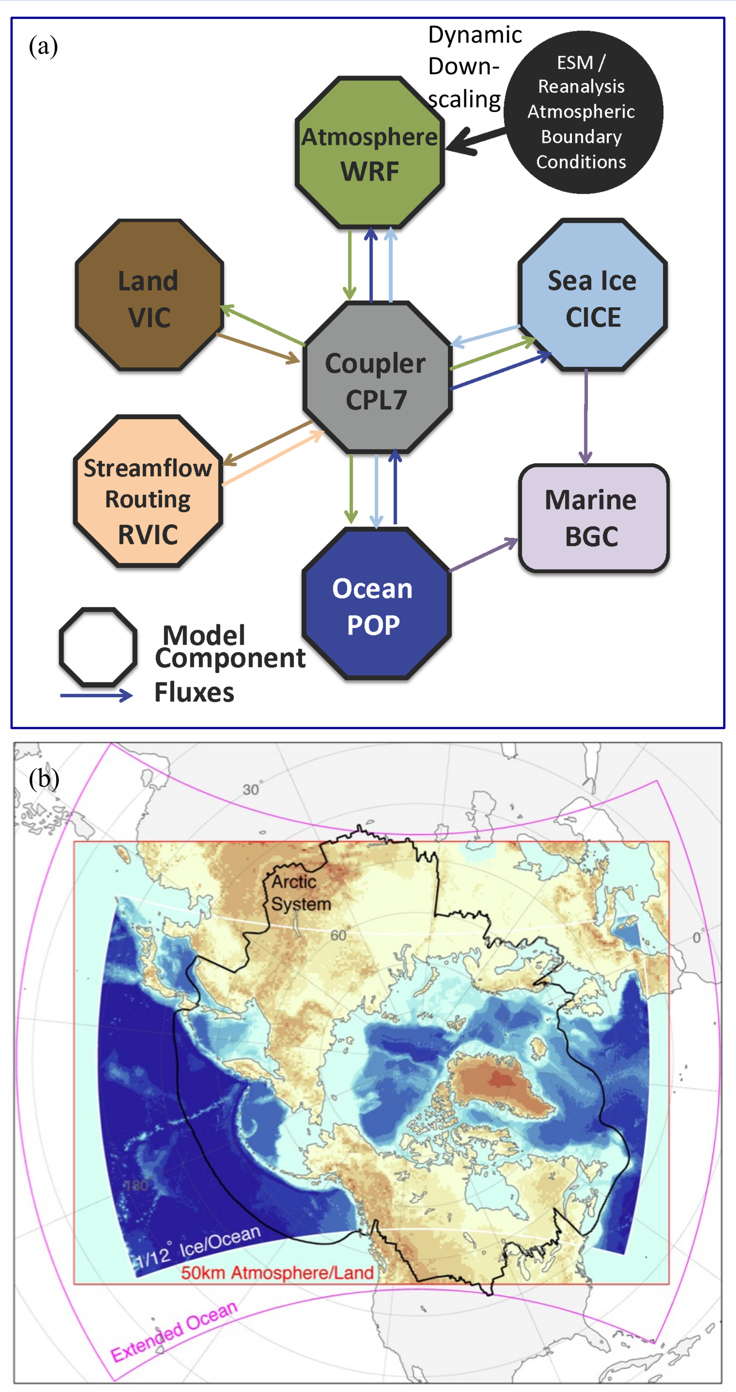

Figure 3. RASM (a) components and wiring diagram and (b) domains and topo-bathymetry.

The RASM is a limited-domain, fully-coupled, high-resolution atmosphere, ocean, ice, and land model. The primary components are the Weather Research and Forecasting (WRF3.7), Los Alamos National Laboratory (LANL) Parallel Ocean Program (POP2) and Sea Ice Model (CICE6), the Variable Infiltration Capacity (VIC) land hydrology model, and a streamflow routing (RVIC) model. These components are coupled using the Community Earth System Model (CESM) coupler (CPL7) (Fig. 3a). The RASM domain includes the Arctic Ocean and surrounding marginal seas as well as the sub-Arctic North Pacific, including the Bering Sea, Sea of Okhotsk, and Gulf of Alaska, and the sub-Arctic North Atlantic, including the Nordic and Labrador seas, Baffin and Hudson bays (Fig. 3b).

3. Sea Ice in CMIP5 vs CMIP6 Models

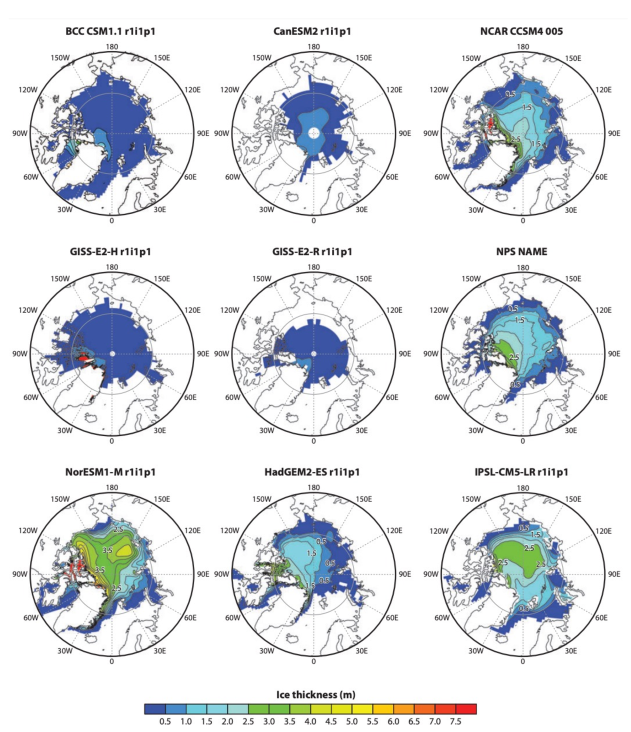

Figure 4. (left) September mean sea ice thickness (m) averaged over 2000-2004 from CMIP5 and NAME models (Fig. 7 in Maslowski et al., 2012)

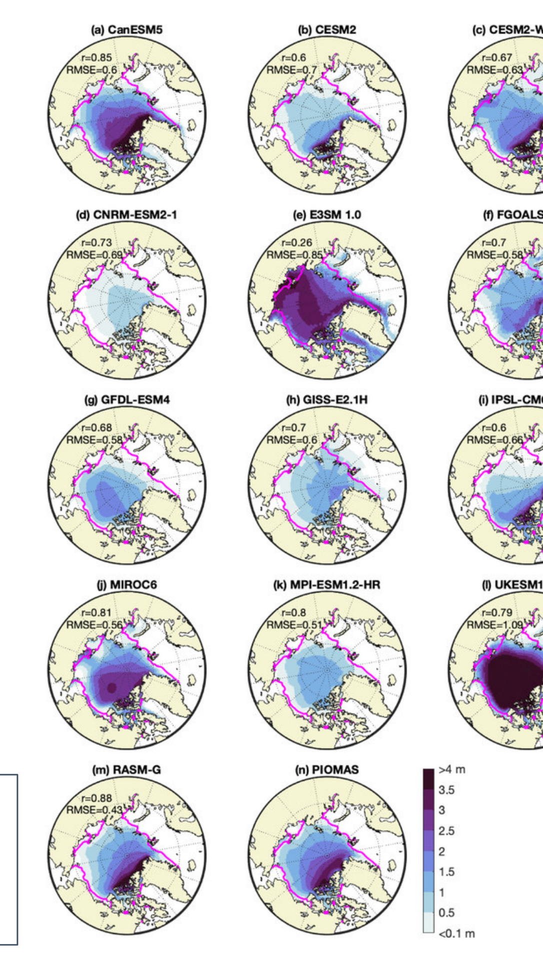

Figure 5. (right) September mean sea ice thickness (m) from CMIP6 and RASM-G simulation (1979–2014) (Fig. 3 in Watts et al. 2012).

❑ **Limitations in, or the absence of, representation of key Arctic physical processes in CMIP5 and CMIP6 models likely contribute to large errors in ice edge and thickness.**

4. Accelerated Sea Ice Decline

❑ **Similar to the CMIP5, all CMIP6 models simulate a decline of sea ice, regardless of their initial conditions, but the accelerated rates appear to vary in intensity between models.**

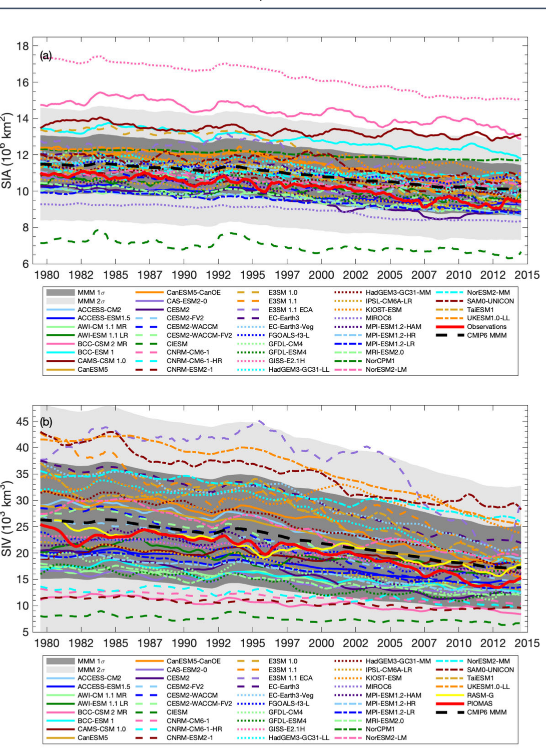

Figure 6. 12-month running mean of (a) SIA and (b) SIV for CMIP6 models. The dark and light gray shadings indicate one and two standard deviation from the observations and multi-model mean (MMM), respectively (Fig. S1 in Lee et al. 2023).

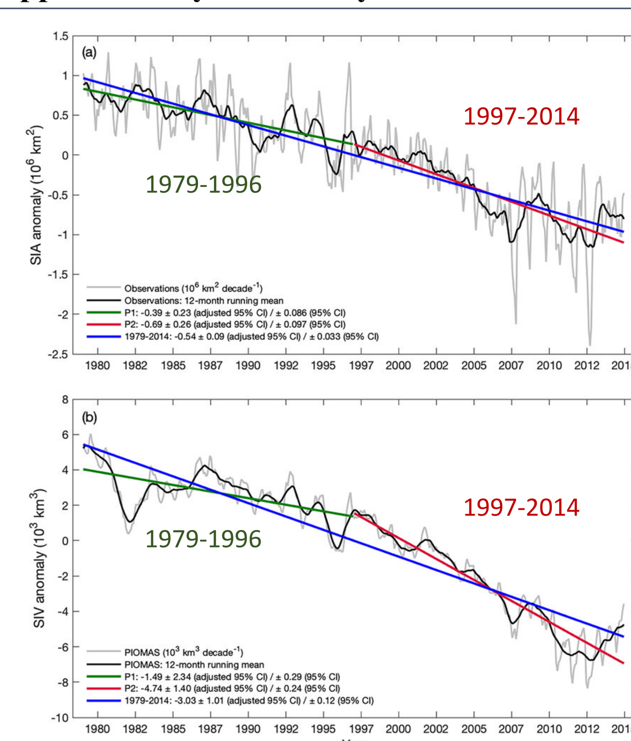

Figure 7. (a) Satellite SIA anomaly (gray), and (b) PIOMAS SIV anomaly (gray) with a . a 12-month running mean (black). The linear regression fits are shown with adjusted 95% confidence intervals (CI) and unadjusted CI (Fig. 1 in Lee et al. 2023).

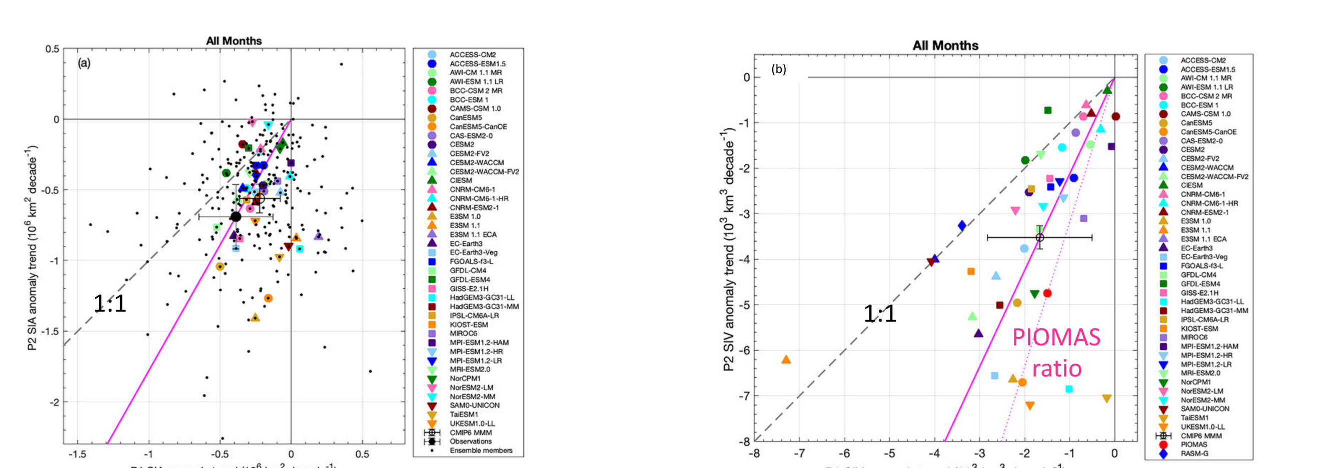

Figure 8. (a) SIA and (b) SIV anomaly trends for 1979–96 (x-axis) and 1997–2014 (y-axis) in the CMIP6 models with the total of 286 ensemble members (black dots) as well as the MMM. The solid magenta lines illustrates the observed SIA and the CMIP6 MMM SIV acceleration ratios, respectively (Figs. 6a and 8a in Lee et al., 2023).

5. The Accelerated Trends of SIA in CMIP6 Models

Model		Full Mean	Full Adj. CI	P1 Mean	P1 Adj. CI	P2 Mean	P2 Adj. CI	Accelerated trend (P2/P1)
ACCESS-CM2	(0/3)	-0.33	0.12	-0.22	0.29	-0.23	0.32	1.04
ACCESS-ESM1.5	(2/20)	-0.37	0.12	-0.20	0.30	-0.33	0.31	1.67
AWI-CM 1.1 MR	(0/5)	-0.37	0.12	-0.18	0.29	-0.46	0.26	2.62
AWI-ESM 1.1 LR	(0/1)	-0.32	0.08	-0.46	0.22	-0.38	0.22	0.83
BCC-CSM 2 MR	(1/3)	-0.52	0.17	-0.29	0.48	-0.63	0.44	2.18
BCC-ESM 1	(1/3)	-0.44	0.12	-0.31	0.36	-0.49	0.27	1.56
CAMS-CSM 1.0	(0/2)	-0.24	0.09	-0.34	0.23	-0.18	0.25	0.52
CanESM5	(7/25)	-0.82	0.12	-0.50	0.28	-1.04	0.26	2.09
CanESM5-CanOE	(1/3)	-0.78	0.18	-0.16	0.28	-1.27	0.23	7.82
CAS-ESM2-0	(0/4)	-0.41	0.09	-0.19	0.27	-0.51	0.21	2.65
CESM2	(0/11)	-0.52	0.16	-0.20	0.37	-0.47	0.47	2.38
CESM2-FV2	(0/3)	-0.49	0.14	-0.08	0.38	-0.52	0.32	6.84
CESM2-WACCM	(0/3)	-0.56	0.13	-0.34	0.32	-0.49	0.37	1.44
CESM2-WACCM-FV2	(0/3)	-0.59	0.13	-0.38	0.32	-0.57	0.40	1.50
CIESM	(0/3)	-0.23	0.11	-0.06	0.33	-0.17	0.25	2.80
CNRM-CM6-1	(1/20)	-0.24	0.11	-0.22	0.28	-0.21	0.29	0.98
CNRM-CM6-1-HR	(0/1)	-0.29	0.09	-0.01	0.23	-0.41	0.24	46.80
CNRM-ESM2-1	(0/5)	-0.35	0.12	-0.25	0.36	-0.38	0.34	1.51
E3SM 1.0	(0/5)	-1.01	0.25	-0.25	0.42	-1.41	0.49	5.56
E3SM 1.1	(0/1)	-0.69	0.16	0.04	0.33	-0.84	0.24	-
E3SM 1.1 ECA	(0/1)	-0.66	0.18	0.19	0.26	-0.83	0.35	-
EC-Earth3	(0/9)	-0.65	0.14	-0.40	0.35	-0.83	0.33	2.06
EC-Earth3-Veg	(2/7)	-0.59	0.14	-0.39	0.29	-0.91	0.26	2.36
FGOALS-f3-L	(0/3)	-0.36	0.12	-0.25	0.26	-0.33	0.31	1.32
GFDL-CM4	(0/1)	-0.49	0.12	-0.52	0.33	-0.76	0.27	1.46
GFDL-ESM4	(0/1)	-0.35	0.11	-0.30	0.45	-0.21	0.18	0.69
GISS-E2.1H	(2/10)	-0.74	0.18	-0.36	0.43	-0.84	0.44	2.34
HadGEM3-GC31-LL	(0/3)	-0.54	0.17	0.06	0.31	-0.92	0.24	-
HadGEM3-GC31-MM	(1/4)	-0.47	0.14	-0.24	0.27	-0.59	0.30	2.39
IPSL-CM6A-LR	(5/32)	-0.54	0.16	-0.31	0.39	-0.57	0.40	1.81
KIOST-ESM	(1/1)	-0.25	0.09	-0.24	0.22	-0.54	0.22	2.28
MIROC6	(1/10)	-0.32	0.09	-0.10	0.19	-0.44	0.24	4.59
MPI-ESM1.2-HAM	(0/3)	-0.38	0.15	0.00	0.40	-0.31	0.35	-
MPI-ESM1.2-HR	(3/10)	-0.41	0.14	-0.26	0.34	-0.51	0.34	1.99
MPI-ESM1.2-LR	(2/10)	-0.36	0.10	-0.24	0.27	-0.40	0.24	1.66
MRI-ESM2.0	(1/5)	-0.43	0.12	-0.29	0.28	-0.38	0.36	1.29
NorCPM1	(2/30)	-0.20	0.08	-0.08	0.18	-0.21	0.18	2.67
NorESM2-LM	(0/3)	-0.25	0.08	-0.27	0.20	-0.02	0.20	0.06
NorESM2-MM	(0/3)	-0.13	0.08	-0.16	0.19	-0.04	0.22	0.23
SAM0-UNICON	(0/1)	-0.42	0.14	-0.02	0.22	-0.90	0.31	49.09
TaiESM1	(0/1)	-0.61	0.15	-0.08	0.24	-0.97	0.41	11.91
UKESM1.0-LL	(4/14)	-0.59	0.12	-0.25	0.26	-0.72	0.24	2.83
CMIP6 SIA MMM		-0.46	0.06	-0.22	0.14	-0.55	0.10	2.55

❑ **Out of 42 CMIP6 models, 17 (40%) models contribute at least one ensemble member toward the 37 skillful simulations of the SIA decline.**

❑ **The likelihood of a skillful simulation increases with the size (i.e., more than 10 ensemble members) of the model ensemble.**

Table 1. Linear trend ($\times 10^6$ km² decade^{-1}) and adjusted 95% confidence interval (adj. CI) of ensemble-mean SIA anomalies for the periods 1979–2014 (Full), 1979–96 (P1), and 1997–2014 (P2). The accelerated trend is the ratio of the P2 trend to the P1 trend. Note that a long dash means a negative (zero) ratio. The boldface font indicates models in which both P1 and P2 trends exhibit no statistically significant difference between simulated and observed SIA and the two trends are statistically different from each other. Parentheses show the number of ensemble members in which P1 and P2 trends and their acceleration are not statistically different from observations (like described above) over the total ensemble members in each CMIP6 model (Table 1 in Lee et al. 2023).

6. Arctic Ocean Heat Transport in CMIP6 Models

❑ **10 out of 18 CMIP6 models show overall positive northward ocean heat transport (OHT) in the high-latitude. The other models exhibit a slightly negative to almost no OHT trend.**

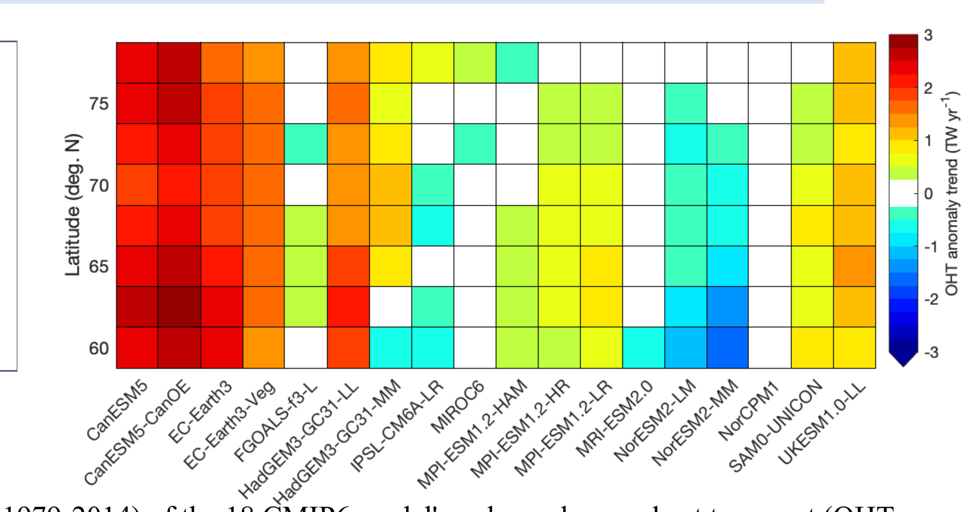

Figure 9. Anomaly trends (TW yr^{-1}; 1979-2014) of the 18 CMIP6 model's poleward ocean heat transport (OHT; *hfbasin*) from 60 to 80 ºN (Fig. S4 in Lee et al. 2023).

7. Emergent Constrain of OHT on Sea Ice Decline

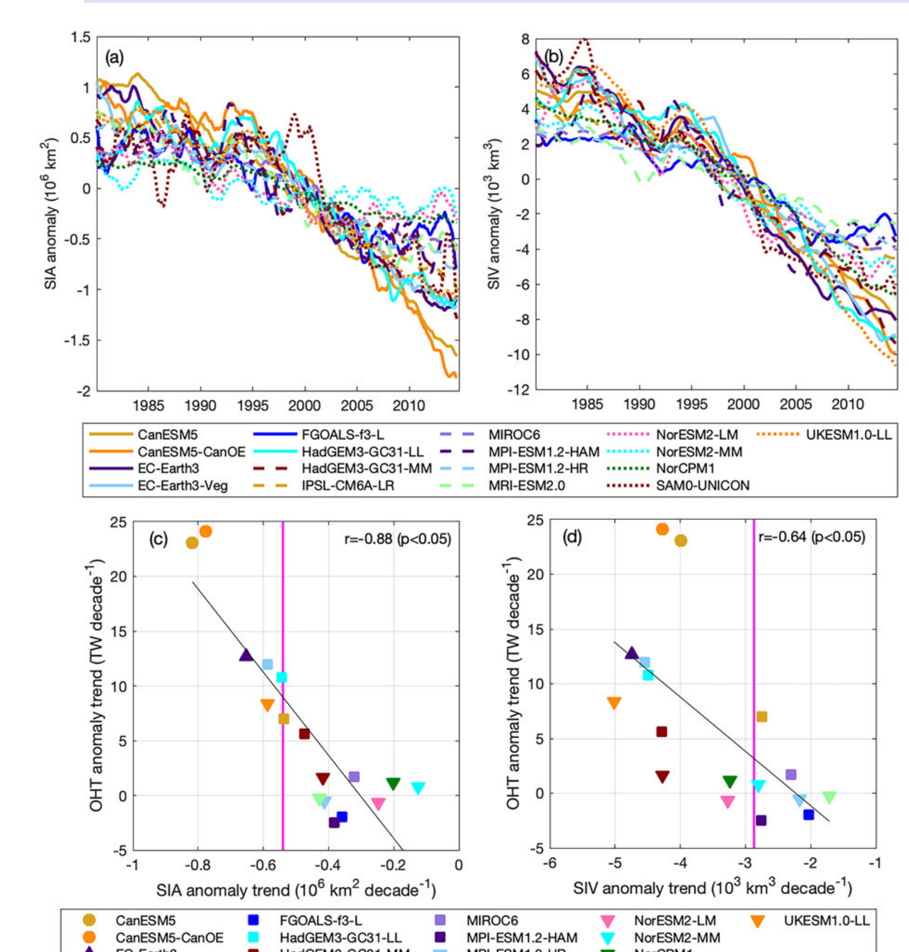

❑ **A strong (r = −0.88; *p*<0.05) relationship is shown between northward OHT anomaly trends at 80ºN and the magnitude of SIA anomaly trends (Fig. 10c)**

❑ **However, the relationship (r = −0.64; *p*<0.05) between OHT anomaly and SIV anomaly trends (Fig. 10d) is not as strong as shown for SIA**

Figure 10. 12-month running mean of (a) SIA and (b) SIV anomaly for 17 CMIP6 models. (c) Scatterplot of northward global ocean heat transport (OHT) anomaly trends at 80°N and pan-Arctic SIA anomaly rends. The magenta line is the satellite observations trend (−0.54 × 10⁶ km2 decade^{-1}). (d) Scatterplot of OHT anomaly trends and pan-Arctic SIV anomaly trends. The magenta line is the CMIP6 MMM trend (−2.87 × 10³ km3 decade^{-1}) (Fig. 9 in Lee et al. 2023).

8. Impact of Oceanic Heat Convergence (OHC) on Sea Ice

❑ **Frazil ice growth reduces (increases) in CMIP6 models with strong positive (negative) OHT trends.**

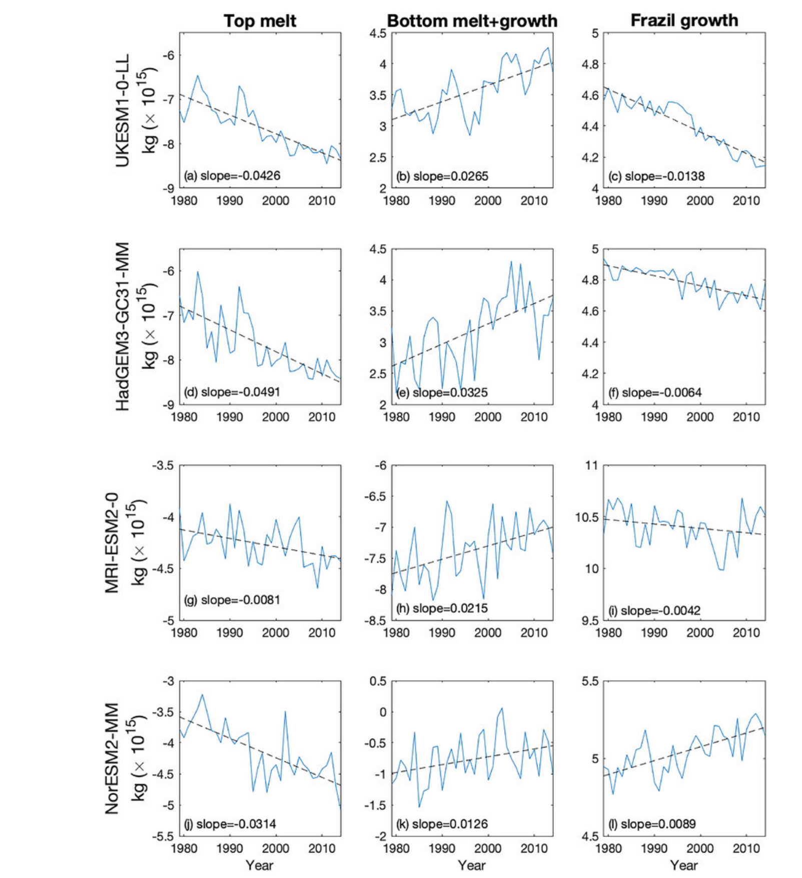

Figure 10. Integrated (a),(d),(g),(j) top melt, (b),(e),(h),(k) bottom sea ice melt and basal growth, and (c),(f),(i),(l) frazil ice growth terms (kg; ×10¹⁵ kg) in UKESM1-0-LL, HadGEM3-GC31-MM, MRI-ESM2-0, and NorESM2-MM, respectively (Fig. 10 in Lee et al. 2023).

❑ **35-40 TW of heat flux into the central Arctic melts sea ice during the summer in the RASM simulation**

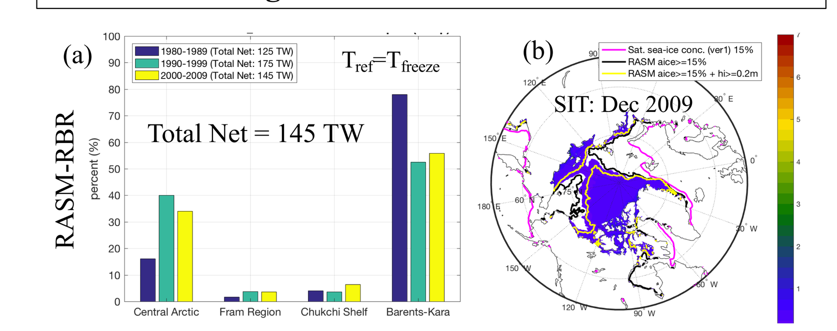

Figure 11. (a) Decadal OHC for the Barents Sea and Central Arctic from RASM sensitivity simulation with dramatically increased OHC into the Central Arctic; (b) Sea ice thickness (SIT) distribution from the end of that RASM simulation in December 2009 showing freshly forming sea ice after the nearly ice-free summer.

9. Summary

1. **Most CMIP6 models show an accelerated decline in both sea ice area and sea ice volume.**
2. **A majority of the CMIP6 models (28 out of 42) underestimate the observed trend of SIA decline.**
3. **A subset of the CMIP6 models (17 out of 42) demonstrates skill in simulating the observed decline and accelerated trends in SIA.**
4. **It requires further process-level investigations into the model simulation of ocean heat transport to better understand its impact on sea ice decline.**
5. **There is a need for more models to submit both OHT and ice mass change for CMIP7 to examine this potential emergent constraint.**

References

Goessling, H. F., Tietsche, S., Day, J. J., Hawkins, E., & Jung, T. (2016). Predictability of the Arctic sea ice edge. *Geophysical Research Letters*, *43*(4), 1642-1650.

Lee, Y. J., Watts, M., Maslowski, W., Kinney, J. C., & Osinski, R. (2023). Assessment of the pan-Arctic accelerated rate of sea ice decline in CMIP6 historical simulations. *Journal of Climate*, *36*(17), 6069-6089.

Maslowski, W., Clement Kinney, J., Higgins, M., & Roberts, A. (2012). The future of Arctic sea ice. *Annual Review of Earth and Planetary Sciences*, *40*, 625-654.

Watts, M., Maslowski, W., Lee, Y. J., Kinney, J. C., & Osinski, R. (2021). A spatial evaluation of Arctic sea ice and regional limitations in CMIP6 historical simulations. *Journal of Climate*, *34*(15), 6399-6420.

Acknowledgments: This work has been supported by the DOE Regional and Global Model Analysis, ONR Arctic and Global Prediction, and DOD High Performance Computing Modernization programs.